Theory of dispersion instabilities associated with surface electromagnetic waves in layered semiconductor media

B. G. Martin
Aerojet ElectroSystems, Azusa, California 91702

R. F. Wallis
Department of Physics, University of California, Irvine, Irvine, California 92717

(Received 7 March 1985)

A theoretical investigation has been made of electromagnetic waves in a two-layer semiconductor system in the presence of a static electric field parallel to the interface. The dispersion relation is obtained using the specular-reflection approach of Kliewer and Fuchs, taking into account retardation and carrier damping. Numerical solutions of the dispersion relation are presented for both retarded and nonretarded cases. These calculations indicate that an interaction takes place between space-charge waves of adjacent media. In some instances, this interaction gives rise to amplifying instabilities. The calculations including retardation show a space-charge-wave—electromagnetic-wave interaction, which results in an evanescent wave localized at the interface.

I. INTRODUCTION

For almost two decades, there has been interest in exploring solid-state plasmas for the various instabilities observed in gaseous plasmas.[1–15] Among the latter, for example, are "resistive-wall" space-charge-wave (SCW) instabilities,[16,17] which have been used for amplifying microwaves. Such instabilities can also occur in solid-state plasmas,[18–20] but their properties have not been extensively investigated.

Consider a metal or a doped semiconductor. SCW's are set up when a static electric field is imposed and the free-charge carriers, electrons, for example, are modulated by an ac electric field. An electron stream is created that has a drift velocity proportional to, and in the direction of, the dc field. The ac modulating field causes variations in the electron number density and, as a consequence, creates SCW's. They arise in pairs, one wave having a phase velocity greater than, and the other having a phase velocity less than, the electron drift velocity. This velocity difference depends on the plasma frequencies, the drift velocities, and the system geometry.[21,22]

It has been observed[16,17] that in the interaction of SCW's with an adjacent resistive medium, amplification of the slow SCW takes place (resistive-wall amplification). The question arises of whether the interaction of SCW's with electromagnetic waves (EMW's) can lead to polariton amplification. Polariton-dispersion theory provides a basic approach for investigating such interactions, as was shown in previous work.[23–26]

In what follows, results are presented on a theoretical investigation of SCW's and EMW's in two contiguous, semi-infinite semiconductor media. The current direction is taken to be parallel to the media interface. An infinitely thin insulating layer is assumed to separate the two semiconductors. The specular-reflection approach of Kliewer and Fuchs[27] is used to satisfy the electromagnetic boundary conditions at the interface and to obtain the dispersion relation. This relation takes into account retardation and spatial dispersion (the wave-vector dependence of the dielectric tensor). Calculated results are presented for a two-layer system, both with and without retardation. The possibilities for mode amplification are explored.

Sturrock's[28] criteria are used for determining whether or not a mode is amplifying. So-called convective and nonconvective instabilities occur in plasmas and are labeled according to whether or not the signs of the group velocities of the interacting modes are the same prior to the interaction. If the group velocities have the same sign, then the interaction can result in a convective instability which is an amplifying wave. If, however, the group velocities have opposite signs, the interaction is nonconvective and not amplifying.

Section II presents the dispersion relation, with retardation, for the two-layer system. Section III gives numerical results and discussion. Conclusions are given in Sec. IV.

II. THEORY

In what follows we consider two semiconductor media containing free-charge carriers that are in contact along a planar interface and are subjected to a static electric field parallel to the interface. The dispersion relation for polaritons localized at the interface is derived using the Kliewer-Fuchs procedure,[27] as mentioned above. Calculated results are presented for several cases of interest.

Specifically, the system consists of one semiconductor with dielectric function $\epsilon_1(\mathbf{k},\omega)$ occupying the half-space $z<0$ and a second semiconductor with dielectric function $\epsilon_2(\mathbf{k},\omega)$ occupying the half-space $z>0$. A static electric field is taken to be in the y direction, as is the direction of propagation of the electromagnetic waves.

The approach used here is essentially that used previously for vacuum-semiconductor systems,[13] i.e., the transport equation for an average carrier is linearized (small-

field approximation) and the elements of the conductivity tensor are obtained. In the absence of thermal-pressure-gradient effects, the result is[14]

$$\sigma_{\alpha\beta}(\mathbf{k},\omega)=\frac{in_0q^2}{m^*\omega}\times\left[(\delta_{\alpha\beta}-\hat{k}_\alpha\hat{k}_\beta)\frac{\beta}{\beta+i\nu}+\frac{(\beta\hat{k}_\alpha+kV_{0\alpha})(\beta\hat{k}_\beta+kV_{0\beta})}{\beta(\beta+i\nu)}\right], \tag{2.1}$$

where $\beta=\omega-\mathbf{k}\cdot\mathbf{V}_0$, $\mathbf{V}_0$ is the drift velocity, and $\hat{k}_\alpha$ is the α component of the unit vector in the $\mathbf{k}$ direction. The quantities n_0, q, m^*, and ν are, respectively, the carrier's density, charge, effective mass, and scattering frequency. The dielectric tensor is related to the conductivity tensor by the relation

$$\epsilon_{\alpha\beta}(\mathbf{k},\omega)=\epsilon_\infty\delta_{\alpha\beta}+\frac{4\pi i}{\omega}\sigma_{\alpha\beta}(\mathbf{k},\omega), \tag{2.2}$$

where ϵ_∞ is the high-frequency background dielectric constant.

Using the specular-reflection approach of Kliewer and Fuchs,[27] one can obtain the dispersion relation for interface modes in the presence of the electric currents in the two media from the electromagnetic boundary conditions. The dispersion relation is found to be

$$0=\int_{-\infty}^{\infty}dk_z\frac{T_{zz}^{(1)}}{T_{yy}^{(1)}T_{zz}^{(1)}-(T_{yz}^{(1)})^2}+\int_{-\infty}^{\infty}dk_z\frac{T_{zz}^{(2)}}{T_{yy}^{(2)}T_{zz}^{(2)}-(T_{yz}^{(2)})^2}, \tag{2.3}$$

where $T_{yy}=(\omega^2/c^2)\epsilon_{yy}-k_z^2$, $T_{yz}=T_{zy}=(\omega^2/c^2)\epsilon_{yz}+k_yk_z$, and $T_{zz}=(\omega^2/c^2)\epsilon_{zz}-k_y^2$. Putting the dielectric tensor components from Eq. (2.2) into Eq. (2.3) and integrating, one obtains the result

$$0=\sum_{s=1}^{2}\frac{\alpha_s\beta_s^2}{\epsilon_\infty^{(s)}[\omega_s^2-\beta_s(\beta_s+i\nu_s)-\epsilon_\infty^{(s)}(\omega_s^2V_s^2/c^2)]^{1/2}[\omega_s^2-\beta_s(\beta_s+i\nu_s)]^{1/2}}, \tag{2.4}$$

where $\omega_s=(4\pi n_sq_s^2/m_s^*\epsilon_\infty^{(s)})^{1/2}$ is the plasma frequency of medium s, $\beta_s=\omega-k_yV_s$, n_s is the carrier concentration, and α_s is the decay constant given by

$$\alpha_s^2=k_y^2+\frac{\epsilon_\infty^{(s)}}{c^2}(\omega_s^2-\omega^2). \tag{2.5}$$

For the nonretarded limit, which gives the dispersion relation for interface SCW's, we take $c=\infty$. In this limit the dispersion relation is a fourth-degree equation in either k_y or ω and, of the resultant four branches, two originate in medium 1 and two in medium 2, as will be discussed below.

The uncoupled dispersion relations (i.e., the bulk SCW dispersion relations in each medium separately) are given, in the nonretarded limit, neglecting damping, by

$$\left[\Omega-\xi\frac{V_s}{V_0}\right]^2=\left[\frac{\omega_s}{\omega_0}\right]^2, \quad s=1,2 \tag{2.6}$$

where $\Omega=\omega/\omega_0$, $\xi=V_0k_y/\omega_0$, ω_0 is a reference plasma frequency, and V_0 is a reference drift velocity. In what follows, the frequency Ω is taken to be real and the wave vector ξ to be complex, i.e., $\xi=\xi_1+i\xi_2$.

It should be mentioned at this point that the nonretarded dispersion relation for the case in which the two media are n- and p-type InSb was discussed some years ago by Steele and Vural.[28] Our dispersion relation, Eq. (2.4), reduces to theirs in the limit $c\to\infty$, $\epsilon_\infty^{(1)}=\epsilon_\infty^{(2)}\to1$, and $\nu_1=\nu_2\to0$.

III. RESULTS AND DISCUSSION

A. SCW dispersion in the nonretarded limit (undamped carriers)

Previous investigations[13,14] were made of a semiconductor with a vacuum interface in the presence of a dc field parallel to the interface. For this system, electromagnetic surface waves occur that are evanescent in character. Now consider replacing the vacuum half-space with a semiconductor having zero drift velocity and described by a Drude dielectric function. The dispersion relation in the nonretarded limit for this configuration is obtained from Eqs. (2.4) and (2.5) simply by taking one drift velocity, say V_2, equal to zero and by letting $c\to\infty$.

Figure 1 shows the dispersion results where the parameters $\omega_0=\omega_1=\omega_2$, $V_0=V_1$, and $\nu_1=\nu_2=0$ were used. The reduced wave vector ξ_1 increases as the frequency increases from zero and becomes infinite at $\Omega=1/\sqrt{2}$. For $\Omega<1/\sqrt{2}$, we have complex-conjugate wave vectors, with one branch (the slow SCW) showing amplification and the other coincident branch (the fast SCW) showing damped behavior. In the case of no carrier damping being considered here, the slow- and fast-SCW branches have the ame Ω-vs-ξ_1 curve for $\Omega<1/\sqrt{2}$; however, the inclusion f damping (see Sec. III B) separates the two branches. It hould be emphasized that the SCW's in Fig. 1 have their lectric and magnetic fields localized at the interface and are therefore interface modes rather than bulk modes.

In the terminology of Sturrock,[29] the slow-SCW branch for $\Omega<1/\sqrt{2}$ is amplified and is said to exhibit a convective instability. This behavior is analogous to that described by Birdsall *et al.*[16,17] for the resistive-wall instabilities mentioned previously.

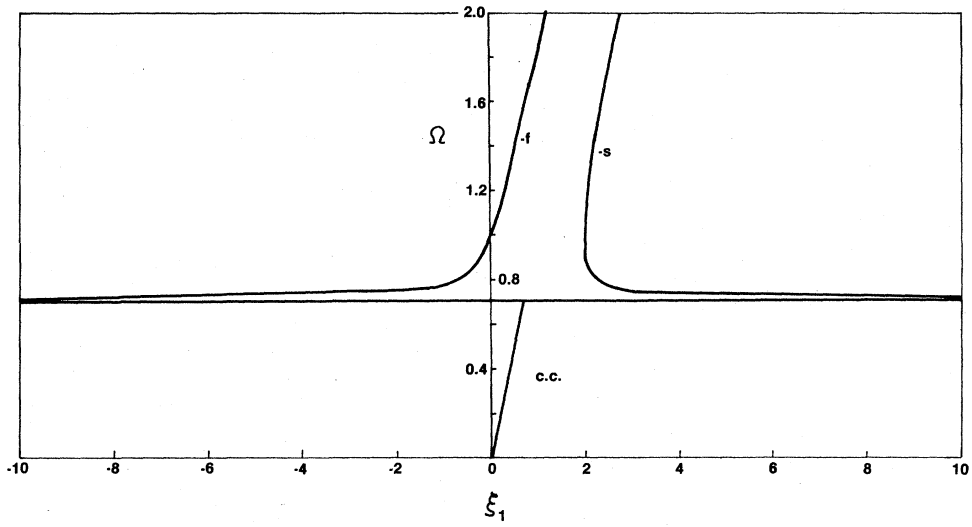

FIG. 1. SCW dispersion curves in the nonretarded limit without damping for $\omega_1=\omega_2=\omega_0$, $V_1=V_0$, and $V_2=0$. f labels the fast branch, s the slow one, c.c. the complex-conjugate wave vectors.

Returning to Fig. 1, we see that for $\Omega > 1/\sqrt{2}$, the slow and fast SCW's are decoupled. With increasing frequency, the slow-SCW wave vector initially decreases rapidly, turns around, and then increases slowly. The fast SCW, on the other hand, has a wave vector that increases with increasing frequency.

Figure 2 shows the frequency dependence of the imaginary part of the wave vector corresponding to the results of Fig. 1. This plot gives the frequency bandwidth of the amplification. In addition, the frequency-dependent gain can be determined from the values of $|\xi_2|$.

Next, consider two semiconductor layers with each having a nonzero drift velocity. Figure 3 shows the resultant SCW dispersion curves given by Eq. (2.6) for $s=1$ and 2. In this situation the two media are decoupled. As indicated in the figure, each medium supports a slow and a fast SCW. In obtaining these results, we have taken $\omega_1=\omega_2=\omega_0$, $V_2/V_0=3$, and $V_1/V_0=1$ so that $V_2/V_1=3$.

Note from Fig. 3 that for frequencies below the point of intersection, the phase velocity of branch b, the fast SCW of medium 1, is greater than the phase velocity of branch c, the slow SCW of medium 2. As long as this condition obtains, there will be an interaction between the slow SCW of the medium having the higher drift velocity and the fast SCW of the medium having the lower drift velo-

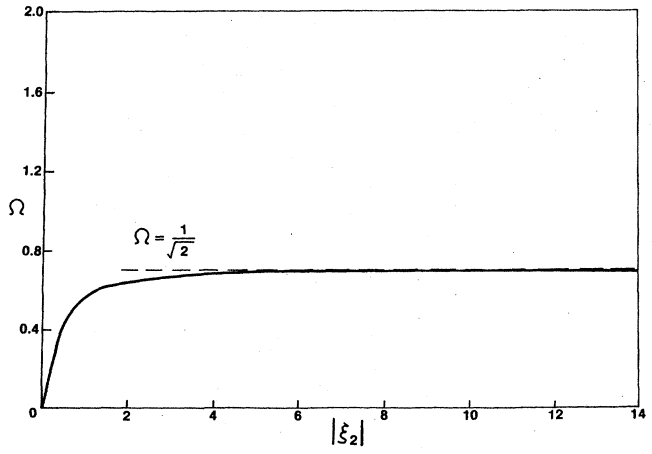

FIG. 2. Imaginary part of the SCW wave vector vs frequency in the nonretarded limit without damping for $\omega_1=\omega_2=\omega_0$ $V_1=V_0$, and $V_2=0$.

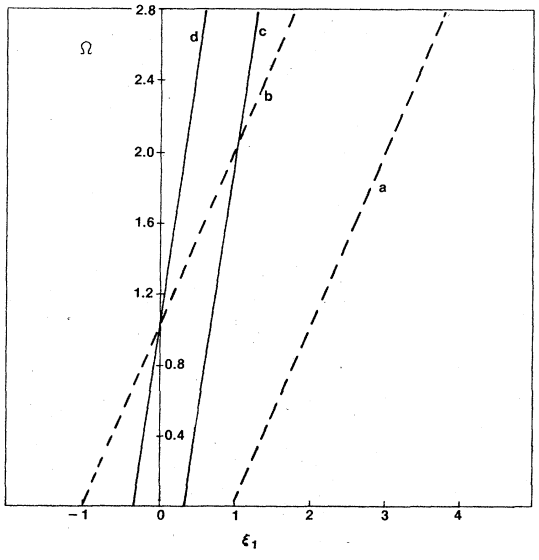

FIG. 3. Uncoupled SCW dispersion curves in the nonretarded limit without damping for $\omega_1=\omega_2=\omega_0$, $V_1=V_0$, and $V_2=3V_0$.

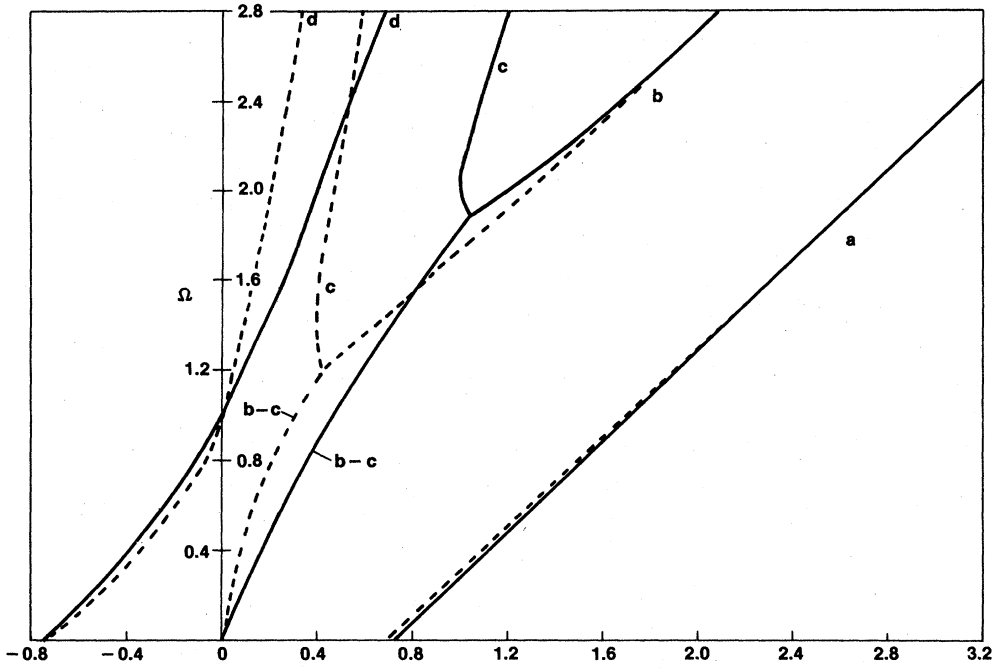

FIG. 4. SCW dispersion curves in the nonretarded limit without damping for $\omega_1=\omega_2=\omega_0$, $V_1=V_0$, and $V_2=3V_0$ (solid curve), $V_2=6V_0$ (dashed curve).

city, giving rise to a convective instability.

Figure 4 shows the coupled dispersion curves obtained by solving Eq. (2.4) for the system of Fig. 3. The *a* and *b* branches still correspond to the slow and fast SCW's in medium 1. Similarly, branches *c* and *d* correspond to the slow and fast SCW's in medium 2. However, for the coupled case, the complete localization of SCW's to a given medium does not occur. Instead, the SCW's are localized at the interface with fields decaying exponentially into each medium with decay constants specified by Eq. (2.5).

Consider first the case $V_2/V_1=3$ of Fig. 4. For branch *a*, the real part of the reduced wave vector increases nearly linearly with frequency, much the same way as in the decoupled case of Fig. 3. Branches *b* and *c* coalesce in the frequency range $0\leq\Omega\lesssim 1.9$, their wave vectors forming a complex-conjugate pair. For this degenerate *b*-*c* branch, the real part of the wave vector, ξ_1, increases with increasing frequency. The *b*-*c* branch is decoupled for frequencies $\Omega\gtrsim 1.9$ and the resultant *b* and *c* branches have a frequency dependence similar to that shown in Fig. 3. Branch *d* has negative values of ξ_1 for $\Omega<1$, crosses the frequency axis at $\Omega=1$ (the plasma frequency), and has positive values of ξ_1 for $\Omega>1$. As this branch crosses the vertical axis from right to left in Fig. 4, it hybridizes with the *b* branch of Fig. 3 and increasingly acquires the character of the *b* branch as ξ_1 becomes increasingly negative.

Consider now the case $V_2/V_1=6$ of Fig. 4. The *a*-branch behavior is nearly coincident with that of $V_2/V_1=3$, except at the lower frequencies. Branches *b* and *c* have complex-conjugate wave vectors for $\Omega\lesssim 1.2$; thus, the frequency range wherein branches *b* and *c* coalesce is shorter than is the case for $V_2/V_1=3$. In other words, increasing the drift-velocity ratio decreases the frequency range of the *b*-*c* degenerate branch. After decoupling, the *b* branch for $V_2/V_1=6$ approaches that of $V_2/V_1=3$. On the other hand, the *c* branch after decoupling moves nearly parallel to the *c* branch for $V_2/V_1=3$, but is displaced toward smaller wave-vector values. The *d* branch for $V_2/V_1=6$ is also displaced from the *d* branch for $V_2/V_1=3$. The reason for the relatively greater displacement of the branches associated with medium 2, as compared with medium 1, is that the reduced drift velocity of the latter was kept fixed at $V_1/V_0=1$, but the reduced drift velocity of medium 2 was increased from 3 to 6.

Figure 5 shows dispersion results for the case in which the drift velocity in medium 1 is opposite that in medium 2, namely, $V_2/V_1=-3$. This situation corresponds to carriers of opposite electrical charge. As before, the plasma frequencies of the two media are equal.

In comparing the dispersive behavior shown in Fig. 5 with that of Fig. 4, a number of differences are evident. Branch *a* of Fig. 5 is a nearly linear function of frequency, as in Fig. 4, but lies in the region of negative wave vectors. This is a consequence of carriers moving in opposite directions. Consider next the *b* and *c* branches. They form a degenerate pair for $0<\Omega\lesssim 0.9$, a consequence of the wave vectors being complex conjugates. This degenerate *b*-*c* branch bends back from positive to negative wave vectors at $\Omega\cong 0.65$. For frequencies $\Omega\gtrsim 0.9$, the *b*-*c* branch decouples, with the *b* branch moving back across the frequency axis nearly parallel to the *d* branch. Note that the frequency range for the unstable *b*-*c* branch is smaller than it is for carriers moving in the same direction (Fig. 4). In terms of the Sturrock criteria the unstable branch of Fig. 5 (*b*-*c*) exhibits a nonconvective insta-

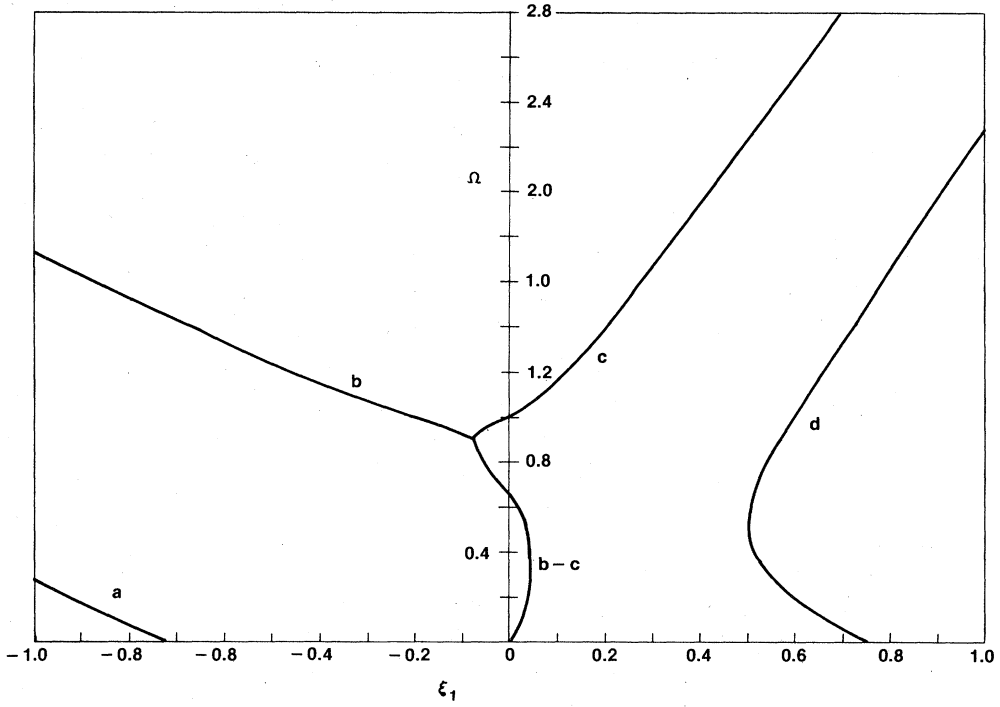

FIG. 5. SCW dispersion curves in the nonretarded limit without damping for $\omega_1=\omega_2=\omega_0$, $V_1=-V_0$, and $V_2=3V_0$.

bility,[28] i.e., a nonamplifying instability.

Figure 6 shows the frequency dependence of the absolute value of $|\xi_2|$, the reduced, imaginary part of the wave vector, for the degenerate b-c branches of Figs. 4 and 5. For all cases, $|\xi_2|$ is zero for $\Omega=0$, increases with Ω to a maximum, and then rapidly decreases, reaching zero again when the branches decouple. Note that the maximum value of $|\xi_2|$, and hence the maximum value

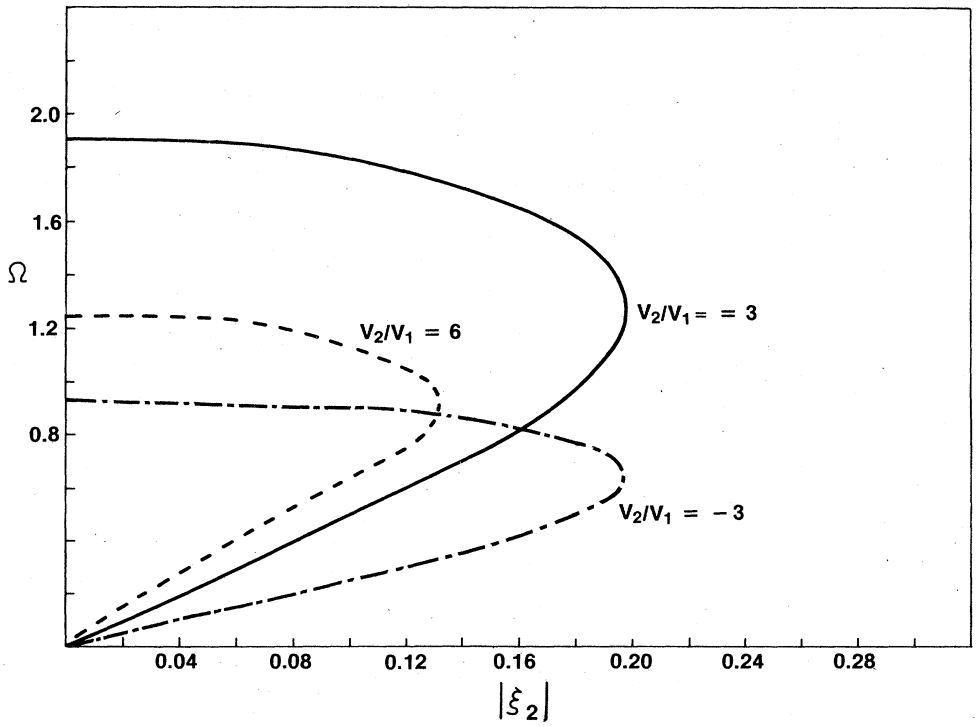

FIG. 6. Imaginary part of the SCW wave vector vs frequency in the nonretarded limit without damping for $\omega_1=\omega_2=\omega_0$ and $V_1=V_0$, $V_2=3V_0$ (solid curve), $V_1=V_0$, $V_2=6V_0$ (dashed curve), and $V_1=-V_0$, $V_2=3V_0$ (dot-dashed curve).

of both slow-SCW amplification and fast-SCW attenuation, is smaller for $V_2/V_1=6$ than for $V_2/V_1=3$. However, the maximum value of $|\xi_2|$ is nearly the same for $V_2/V_1=3$ as it is for $V_2/V_1=-3$. For the latter case, which is not amplifying, the maximum $|\xi_2|$ occurs at the frequency where, in Fig. 5, the degenerate b-c branch has $\xi_1=0$, i.e., the SCW's have infinite phase velocity.

The above results indicate that the SCW coupling and resultant instability are a function of the drift-velocity ratio of the media. Table I shows the effect of the drift-velocity ratio on parameters characterizing the SCW instability.

From Table I we note that the maximum amplification of the slow SCW, as well as the maximum attenuation of the fast SCW, increases with decreasing drift-velocity ratio. This trend continues until $V_2/V_1=1$, at which point there is no SCW interaction, i.e., the imaginary part of each wave vector goes to zero. The bandwidth decreases rapidly as the drift-velocity ratio moves away from unity. The frequency at which the maximum in $|\xi_2|$ occurs increases substantially with decreasing drift-velocity ratio, as does the cutoff frequency.

In addition to the drift-velocity-ratio effects discussed above, the effect of media plasma-frequency differences on SCW instability was investigated. Table II gives some data on the effect of plasma-frequency variations on the maximum slow-SCW gain, neglecting carrier damping. The drift-velocity ratio V_2/V_1 was kept fixed at 3. The data of Table II show that the maximum gain increases essentially linearly with increasing plasma frequency when $\omega_1/\omega_0=\omega_2/\omega_0$. The frequency Ω at which the gain is maximum also increases essentially linearly with plasma frequency.

Keeping the plasma frequency ω_2 fixed (the plasma frequency of the medium with the higher drift velocity) and increasing ω_1 also results in an increase in gain, as well as an increase in the frequencies at which the maximum gain occurs. However, the gain increase is not as great as when both ω_1 and ω_2 are increased. Similar behavior occurs when ω_I is kept fixed and ω_2 is increased.

TABLE I. Approximate values of maximum gain and bandwidth vs drift-velocity ratio for the case of no damping with $V_1=V_0$ and $\omega_1=\omega_2=\omega_0$.

$\frac{V_2}{V_1}$	$(\xi_2)_{\max}$	Bandwidth (units of ω/ω_0)
0	∞	0.71
0.2	0.74	1.4
0.4	0.55	2.3
0.6	0.46	3.4
0.8	0.40	9.0
1.0	0	
1.2	0.33	11
1.4	0.30	6.0
1.6	0.28	4.3
2.0	0.25	3.0
3.0	0.20	2.0
4.0	0.17	1.6
5.0	0.15	1.4
6.0	0.13	1.3
8.0	0.12	1.2
10	0.10	1.1
∞	0	

TABLE II. Effect of plasma-frequency variations on the maximum gain of slow SCW's when carrier damping is neglected, $V_1=V_0$ and $V_2=3V_0$.

$\frac{\omega_1}{\omega_0}$	$\frac{\omega_2}{\omega_0}$	$\lvert\xi_2\rvert_{\max}$	Ω (at max)
1	1	0.20	1.3
2	2	0.39	2.6
4	4	0.79	5.0
2	1	0.26	2.3
4	1	0.35	4.4
1	2	0.29	1.5
1	4	0.41	2.1

B. SCW dispersion for damped carriers in the nonretarded limit

Figure 7 presents dispersion curves for the situation in which carrier damping is taken into account; specifically, we consider the damping parameter values $\nu_1=\nu_2=0.1\omega_0$. We take the drift-velocity ratio $V_2/V_1=3$ and the plasma frequencies ω_1 and ω_2 to be equal.

Consider branch a of Fig. 7. Its linear dependence on frequency and its relative position remain substantially unchanged by the imposition of damping (compared to Fig. 4). Likewise, branch-d dispersion remains essentially unaffected by carrier damping. The interaction of branches b and c, however, differs in one noticeable aspect from the case in which there is no damping, namely, the degeneracy of these branches for $\Omega<1.9$ is removed and the wave vectors, though complex, are no longer complex conjugates. Relatively large values of ν_1 and ν_2 were used to make the removal of the degeneracy evident in Fig. 7. In the frequency range $0<\Omega<1.9$, the c-branch SCW (slow SCW) has a negative imaginary part of the wave vector which corresponds to an amplifying wave. The b-branch SCW (fast SCW), on the ohter hand, has a positive imaginary part of the wave vector, corresponding to an attenuating SCW. The frequency at which amplification of the c-branch SCW ceases is $\Omega\cong1.9$.

Figure 8 gives the frequency dependence of $|\xi_2|$ associated with the dispersion curves of Fig. 7. Consider first the $c(-)$ branch which corresponds to the amplified SCW. Its frequency dependence is qualitatively similar to that corresponding to $V_2/V_1=3$ in Fig. 6. Quantitatively, the inclusion of damping decreases the maximum gain and increases slightly the frequency range of amplification. The $c(-)$ branch terminates at $\Omega=2$, and for $\Omega>2$ the $c(+)$ branch represents an exponentially attenuating SCW. Note from the figure that Ω increases rapidly with increasing $|\xi_2|$ for the $c(+)$ branch.

The a, b, and d branches of Fig. 8 are for SCW's that are exponentially attenuating in the direction of propaga-

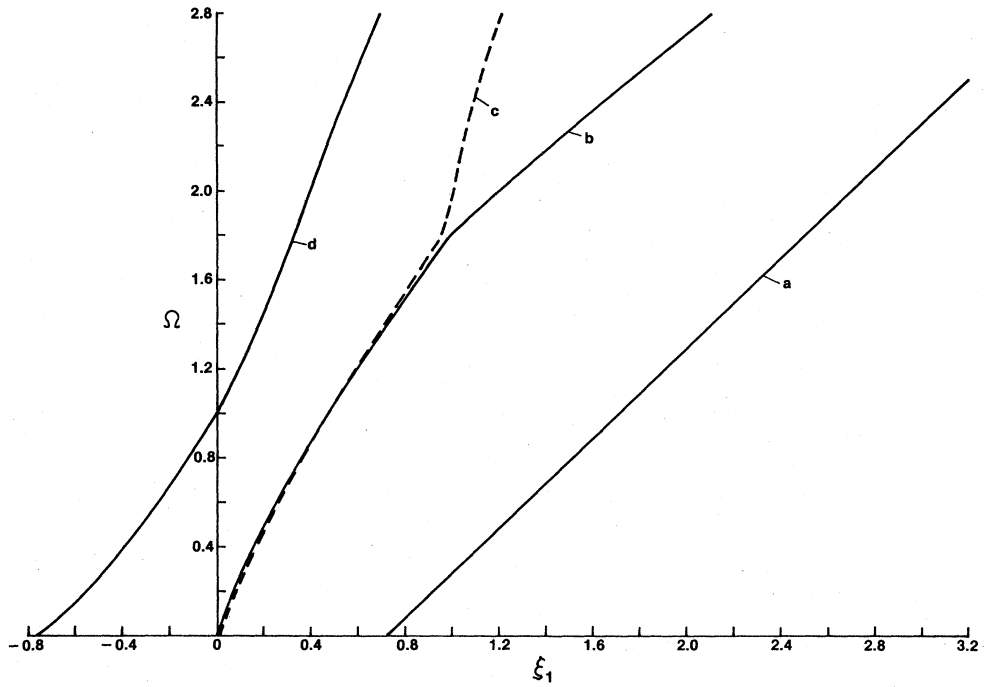

FIG. 7. SCW dispersion curves in the nonretarded limit with carrier damping included for $\omega_1=\omega_2=\omega_0$, $\nu_1=\nu_2=0.1\omega_0$, $V_1=V_0$, and $V_2=3V_0$.

tion. For the a branch, $|\xi_2|$ is relatively independent of Ω. For the b branch, $|\xi_2|$ increases with Ω, reaches a maximum at $\Omega\cong 1.3$, and then rapidly decreases with Ω until $\Omega\cong 2$, at which point it begins to slowly approach the same asymptotic value as the a branch. Finally, the d branch is somewhat more frequency dependent than the a branch, but not as much as the b and c branches. At $\Omega=0$, the d branch is nearly coincident with the a branch, and as $\Omega\rightarrow\infty$ it approaches the same asymptotic value as the $c(+)$ branch.

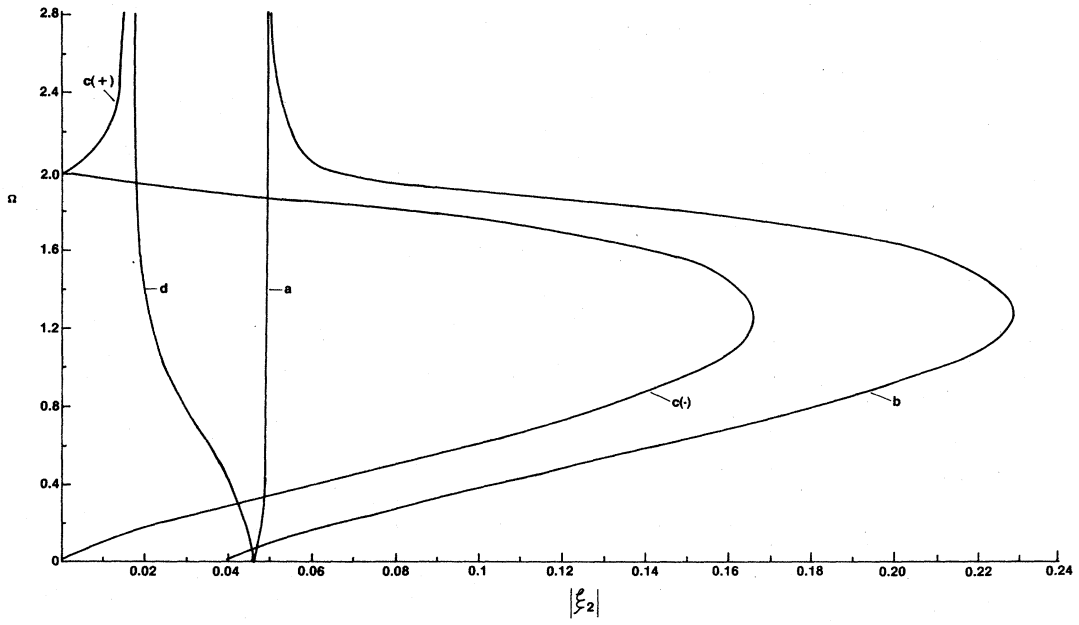

FIG. 8. Imaginary part of the SCW wave vector vs frequency in the nonretarded limit with carrier damping included for $\omega_1=\omega_2=\omega_0$, $\nu_1=\nu_2=0.1\omega_0$, $V_1=V_0$, and $V_2=3V_0$. The labeling of the curves is explained in the text.

C. SCW dispersion including retardation

Dispersion results have been obtained when retardation is taken into account for two media with different plasma frequencies, but carrier damping is excluded. Making the plasma frequencies different introduces interface modes (IFM's).[30] The dispersion relation for interface modes in the absence of drift currents is[30]

$$\sum_{s=1}^{2} \frac{\alpha_s}{\epsilon_\infty^{(s)}(\omega_s^2-\omega^2)}=0 , \tag{3.1}$$

where α_s is given by Eq. (2.5) and specifies the decay of the electric and magnetic fields into medium s. The IFM dispersion curve is asymptotic to the frequency specified by $\omega^2=\frac{1}{2}(\omega_1^2+\omega_2^2)$. In Fig. 9 we present the IFM dispersion curve for the case $\epsilon_\infty^{(1)}=\epsilon_\infty^{(2)}=11.7$ (silicon), $\omega_1/\omega_0=1$, and $\omega_2/\omega_0=\sqrt{2}$.

When drift velocities are imposed on the two media, the IFM becomes Doppler shifted and acquires the character of a SCW. The introduction of retardation causes an interaction between the Doppler-shifted IFM and electromagnetic waves leading to Doppler-shifted interface polaritons. Figure 10 shows the resulting dispersion curves obtained from Eq. (2.4) for the same parameters as Fig. 9, but with drift velocities $V_1=0.0015c$ and $V_2=0.0005c$. For this situation, the interaction leads to not only an interface polariton (branch 1), but also to branch d-1 which is degenerate with complex-conjugate wave vectors. With increasing frequency, this degenerate branch moves rapidly toward small wave-vector values and finally terminates (see figure insert). A Sturrock[30] analysis of this degenerate branch reveals that it is an evanescent wave. It is reminiscent of the behavior investigated previously[14] of a single current-bearing medium against vacuum.

The branch-2 interface polariton of Fig. 10 no longer shows the asymptotic behavior it exhibited in the uncoupled case of Fig. 9. Instead, it acquires the character of the SCW d branch of Fig. 4 at large positive wave vectors. The SCW branches a, b, and c are essentially unaffected by the introduction of different plasma frequencies and retardation. The degenerate b-c branch still has convective instability.

Figure 11 shows SCW and IFM interactions where the carriers in one medium are moving in a direction opposite to those in the other medium. Recall that Fig. 5 showed the results for this situation, neglecting retardation and IFM's.

The a and d branches of Fig. 11 show behavior similar to that of Fig. 5, as does the b-c degenerate branch. In addition, the IFM branch 2 behaves essentially as it does for the situation shown in Fig. 10. However, there are a number of features in Fig. 11 that are different from their counterparts in Fig. 10. For example, the b-c degenerate branch crosses both the 1 and 2 IFM branches for frequencies $\Omega\cong 1.08$. In this crossing there is no evidence of a SCW-IFM interaction. At $\Omega\cong 1$, the b-c degenerate branch decouples and, with increasing frequency, the wave vector associated with the b branch increases. With increasing frequency the c branch rapidly moves to the right and then couples with the IFM branch 1, forming the c-1 degenerate branch, which quickly moves in toward the frequency axis. For reduced wave vectors $\xi_1<1$, the c-1 degenerate branch behaves in a way similar to that shown in the inset of Fig. 10, except that it crosses the Ω axis and moves nearly vertically, but slightly to the right of the Ω axis.

Table III lists decay constants [Eq. (2.5)] corresponding to Fig. 10 for selected frequencies. Note that for SCW branches a, b, and c, the decay constants α_1 and α_2 are identical for all the frequencies considered. This is because the wave-vector contribution is dominant in Eq. (2.5). In other words, $\alpha_1=\alpha_2=k_y$. For the SCW d branch, however, $\alpha_1\neq\alpha_2\neq k_y$ for frequencies $\Omega>1.1$. In this case, the wave vector is not dominant. Finally, for

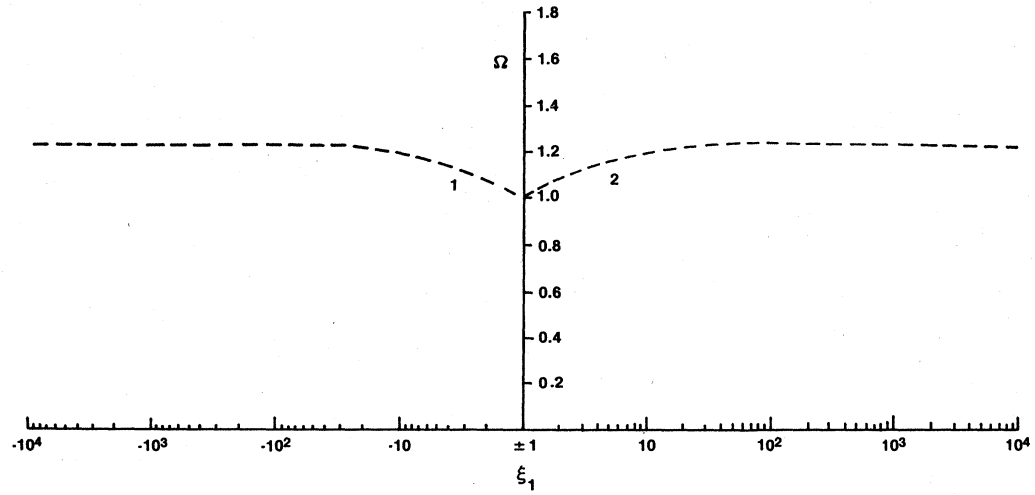

FIG. 9. Interface-mode dispersion curves including retardation but without damping for $\omega_1=\omega_0$, $\omega_2=\sqrt{2}\omega_0$, and $V_1=V_2=0$.

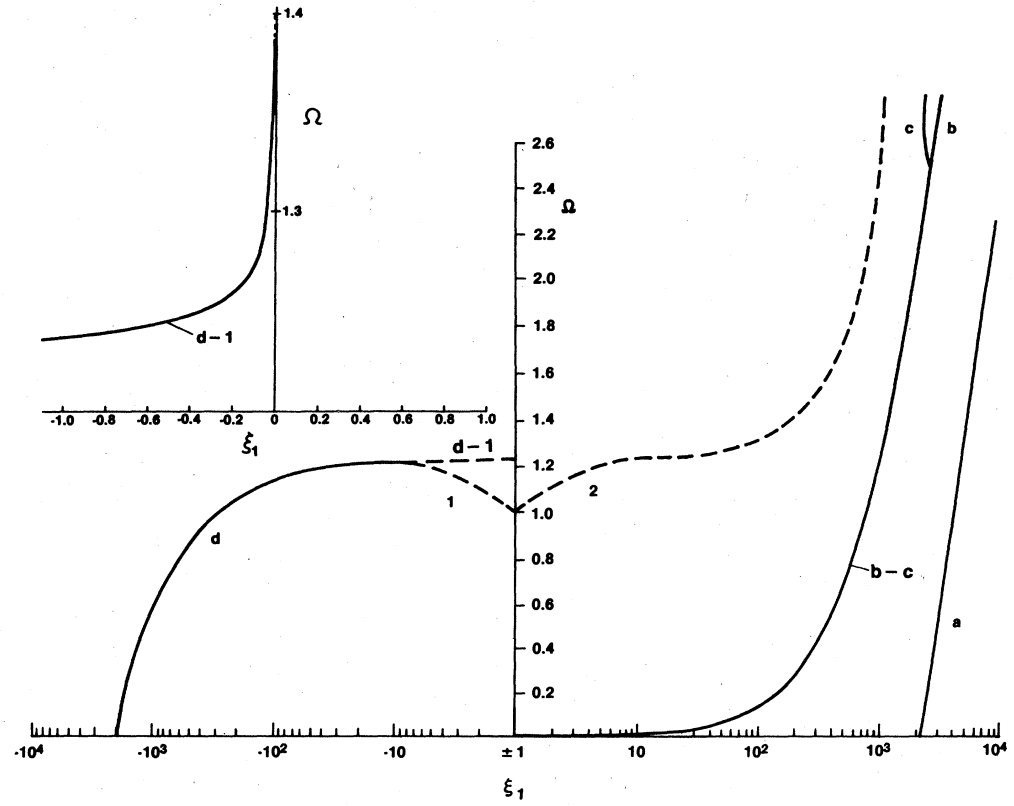

FIG. 10. Retarded dispersion curves without damping for $\omega_1=\omega_0$, $\omega_2=\sqrt{2}\omega_0$, $V_1=0.0015c$, and $V_2=0.0005c$.

the d-1 degenerate branch, the real parts of α_1 and α_2 decrease with increasing frequency, i.e., the corresponding electromagnetic waves become less and less localized near the interface. Similar behavior is observed for the c-1 branch of Fig. 11.

IV. CONCLUSIONS

An investigation has been made of SCW and EMW interactions in layered semiconductor media. Calculations both without and with carrier damping were made. For the former case, calculations were made both without and with retardation.

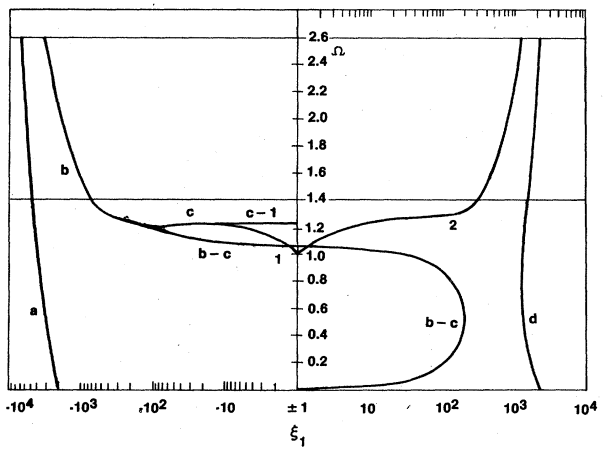

FIG. 11. Retarded dispersion curves without damping for $\omega_1=\omega_0$, $\omega_2=\sqrt{2}\omega_0$, $V_1=-0.0015c$, and $V_2=0.0005c$.

SCW's in media with different drift velocities but with carriers of the same charge can interact, giving rise to an amplifying slow SCW and a decaying fast SCW. The amplification of the slow SCW decreases with increasing drift-velocity ratio $V_2/V_1\neq 1$ (when $V_2=V_1$, there is no SCW interaction). The frequency at which the maximum amplification occurs decreases with increasing drift-velocity ratio. The frequency range of amplification decreases with increasing drift-velocity ratio. Systems in which the current carriers in one medium drift in the direction opposite to those in the adjacent medium have their maximum values of $|\xi_2|$ for a given drift-velocity ratio at a lower frequency than do systems in which the carriers drift in the same direction.

The imposition of carrier damping decreases the slow-SCW amplification and increases the frequency range of amplification, but has no effect on the frequency at which the maximum amplification takes place.

Finally, when retardation is included for the case in which the two media have different plasma frequencies, an interaction takes place between an interface polariton and a fast SCW. The resultant wave is evanescent. The same is true for the case of carriers in one medium drifting opposite to those in the other medium.

There is an obvious attraction to exploiting SCW instabilities for making solid-state amplifiers or oscillators. An investigation is being made of basic design parameters

TABLE III. Decay constants for the retarded case with $V_1=0.0015c$, $V_2=0.0005c$, $\omega_1=\omega_0$, $\omega_2=\sqrt{2}\omega_0$, and $\nu_1=\nu_2=0$. The mode indices correspond to those in Fig. 10.

Ω	Mode	$\frac{c\alpha_1}{\omega_0}$ (real, imag.)	$\frac{c\alpha_2}{\omega_0}$ (real, imag.)
1.1	1	0.972, 0	3.56, 0
	2	0.915, 0	3.54, 0
	a	4.22×10^3, 0	4.22×10^3, 0
	b	9.03×10^2, $+3.54\times10^2$	9.03×10^2, $+3.54\times10^2$
	c	9.03×10^2, -3.54×10^2	9.03×10^2, -3.54×10^2
	d	1.57×10^2, 0	1.57×10^2, 0
1.2	1	4.96, 0	6.02, 0
	2	3.94, 0	5.22, 0
	a	4.42×10^3, 0	4.42×10^3, 0
	b	1.01×10^3, $+3.83\times10^2$	1.01×10^3, $+3.83\times10^2$
	c	1.01×10^3, -3.83×10^2	1.01×10^3, -3.83×10^2
	d	29.0, 0	29.2, 0
1.3	1	0.021, 3.83	0.046, 1.72
	2	87.7, 0	87.8, 0
	a	4.62×10^3, 0	4.62×10^3, 0
	b	1.11×10^3, $+4.09\times10^2$	1.11×10^3, $+4.09\times10^2$
	c	1.11×10^3, -4.09×10^2	1.11×10^3, -4.09×10^2
	d	0.021, -3.83	0.046, -1.72
1.4	1	1.58×10^{-4}, 3.42	3.79×10^{-3}, 0.143
	2	1.97×10^2, 0	1.97×10^2, 0
	a	4.81×10^3, 0	4.81×10^3, 0
	b	1.23×10^3, $+4.29\times10^2$	1.23×10^3, $+4.29\times10^2$
	c	1.23×10^3, -4.29×10^2	1.23×10^3, -4.29×10^2
	d	1.58×10^{-4}, -3.42	3.79×10^{-3}, -0.143
2.4	1	0, 5.58	0, 4.41
	2	1.04×10^3, 0	1.04×10^3, 0
	a	6.8×10^3, 0	6.8×10^3, 0
	b	2.48×10^3, $+1.44\times10^2$	2.48×10^3, $+1.44\times10^2$
	c	2.48×10^3, -1.44×10^2	2.48×10^3, -1.44×10^2
	d	0, -5.58	0, -4.41
2.5	1	0, 5.83	0, 4.72
	2	1.12×10^3, 0	1.12×10^3, 0
	a	7.01×10^3, 0	7.01×10^3, 0
	b	2.80×10^3, 0	2.80×10^3, 0
	c	2.41×10^3, 0	2.41×10^3, 0
	d	0, 5.82	0, 4.72
2.6	1	0, 6.1	0, 5.0
	2	1.19×10^3, 0	1.19×10^3, 0
	a	7.21×10^3, 0	7.21×10^3, 0
	b	6.64×10^2, 0	6.64×10^2, 0
	c	3.06×10^3, 0	3.06×10^3, 0
	d	0, -6.1	0, -5.0

needed to determine the practicality of SCW devices utilizing GaAs-$Ga_xAl_{1-x}As$ heterostructures, prepared by molecular-beam epitaxy, in which very high mobilities in the GaAs layer can be attained. One design[31] presently being investigated involves a high electron mobility transistor (HEMT) —inverted-HEMT structure when the electron drift velocity in the HEMT channel is greater by a factor of 2—5 than that in the inverted HEMT channel. The close proximity of the two electron channels assures the interaction of the space-charge waves.

ACKNOWLEDGMENT

The work of one of the authors (R.F.W.) was supported by National Science Foundation Grant No. DMR-82-14214.

[1]G. A. Baraff and S. J. Buchsbaum, Phys. Rev. **144**, 266 (1966).
[2]G. S. Kino, Appl. Phys. Lett. **12**, 312 (1968).
[3]B. E. Burke and G. S. Kino, Appl. Phys. Lett. **12**, 310 (1968).
[4]S. I. Khankina and V. M. Yakovenko, Fiz. Tverd. Tela (Leningrad) **9**, 2943 (1967) [Sov. Phys.—Solid State **9**, 2312 (1968)].
[5]A. Bers and B. E. Burke, Appl. Phys. Lett. **16**, 300 (1970).
[6]C. Kirscher and A. Bers, Appl. Phys. Lett. **18**, 349 (1971).
[7]Dinesh Chandra Tiwari and J. S. Verma, Indian J. Pure Appl. Phys. **13**, 772 (1975).
[8]N. N. Beletskii and V. M. Yakovenko, Fiz. Tekh. Poluprovodn. **9**, 554 (1975) [Sov. Phys.—Semicond. **9**, 364 (1975)].
[9]N. L. Pandey and R. N. Singh, Phys. Rev. B **14**, 719 (1976).
[10]S. Guha and P. K. Sen, J. Phys. D **10**, 1951 (1977).
[11]T. Tajima and S. Ushioda, Phys. Rev. B **18**, 1892 (1978).
[12]B. G. Martin, A. A. Maradudin, and R. F. Wallis, Surf. Sci. **19**, 37 (1980).
[13]B. G. Martin, J. J. Quinn, and R. F. Wallis, in Proceedings of the Fourth International Conference on Solid Surfaces, Cannes, France, 1980 (unpublished).
[14]B. G. Martin, J. J. Quinn, and R. F. Wallis, Surf. Sci. **105**, 145 (1981).
[15]J. Pozhela, *Plasma and Current Instabilities in Semiconductors* (Pergamon, Oxford, 1981).
[16]C. K. Birdsall, G. R. Brewer, and A. V. Haeff, Proc. IRE **41**, 865 (1953).
[17]C. K. Birdsall and J. R. Whinnery, J. Appl. Phys. **24**, 314 (1953).
[18]Akira Hasegawa, J. Phys. Soc. Jpn. **20**, 1072 (1965).
[19]S. I. Khankina and V. M. Yakovenko, Fiz. Tverd. Tela (Leningrad) **9**, 578 (1967) [Sov. Phys.—Solid State **9**, 443 (1967)].
[20]Yoshihiko Mizushima and Tsuneta Sudo, IEEE Trans. Electron Devices **ED-17**, 541 (1970).
[21]A. H. W. Beck, *Space Charge Waves and Slow Electromagnetic Waves* (Pergamon, Oxford, 1958).
[22]J. R. Pierce, *Almost All About Waves* (MIT, Cambridge, Mass., 1974).
[23]R. F. Wallis, B. G. Martin, and J. J. Quinn, in Proceedings of the 16th International Conference on the Physics of Semiconductors, Montpelier, France, 1982 (unpublished).
[24]B. G. Martin, R. F. Wallis, and J. J. Quinn, Bull. Am. Phys. Soc. **28**, 858 (1983).
[25]B. G. Martin and R. F. Wallis, J. Phys. (Paris) **45**, C5-255 (1984).
[26]B. G. Martin and R. F. Wallis, Bull. Am. Phys. Soc. **29**, 478 (1984).
[27]K. L. Kliewer and R. Fuchs, Phys. Rev. **172**, 608 (1968).
[28]M. C. Steele and B. Vural, *Wave Interactions in Solid State Plasmas* (McGraw-Hill, New York, 1969).
[29]P. A. Sturrock, Phys. Rev. **112**, 1488 (1958).
[30]P. Halevi, Phys. Rev. B **12**, 4032 (1975).
[31]This design was the result of collaboration with C. Shannon and I. Galin of Aerojet ElectroSystems, Azusa, CA.